Facilitated Dissociation of Nucleoid Associated Proteins from DNA in the Bacterial Confinement

Zafer Koşar[1], A. Göktuğ Attar[2], and Aykut Erbaş[1]
[1] *UNAM-National Nanotechnology Research Center and Institute of Materials Science & Nanotechnology, Bilkent University, Ankara 06800, Turkey and*
[2] *Department of Molecular Biology & Genetics, Bilkent University, Ankara 06800, Turkey*

Transcription machinery ultimately depends on the temporal formation of protein-DNA complexes. Recent experimental studies demonstrate that residence time (i.e., inverse off-rate) of a transcription factor protein can be a contributor to the functional diversity of the protein. In the meantime, single-molecule experiments showed that the off-rates of a wide array of DNA-binding proteins accelerate as the bulk concentration of the protein increases via a concentration-dependent mechanism (i.e., facilitated dissociation, FD). In this study, inspired by the previous single-molecule studies on the factor for inversion stimulation (Fis) protein of *E. coli*, which is a dual-purpose protein with a diverse functionality, we model the unbinding of Fis from specific bindings sites along a high-molecular-weight circular DNA in a cylindrical structure mimicking the cellular confinement of chromosome. Our simulations show that FD of Fis can well occur in confinement at physiological concentrations. Particularly, when nutrient-rich conditions are emulated with Fis concentrations around micromolar levels, the off-rates increase one order of magnitude compared to the lower Fis levels. However, Fis significantly changes the chromosome structure at higher concentrations by forming dense protein clusters bridging specific sites and juxtaposing remote DNA segments. As a result, at the physiologically observed maximum levels of Fis, the off-rates significantly slow down. Overall, our results indicate that cellular-concentration levels of a structural DNA-binding protein is intermingled with the genome architecture and DNA residence times, thereby providing a basis for understanding the complex effects of dynamic protein-DNA interactions on gene regulation.

I. INTRODUCTION

Bacterial transcription factors (TFs) are DNA-binding proteins that can dynamically regulate RNA polymerase's involvement in the transcription machinery by transiently binding to DNA [1, 2]. The formation of a DNA-TF complex upon binding is often considered sufficient for the biomolecular functionality of the corresponding TF (i.e., activation or repression of the target gene) [3]. However, a growing body of work has demonstrated that the time that a TF spends along the genome (i.e., residence time) could regulate the TF functions, and this effect is more dramatic if the TF has diverse biological functionality [4–6]. Independently, the recent *in vitro* single-molecule experiments show that off-rates (i.e., reciprocal of the residence time) of major bacterial TF proteins, including the factor for inversion stimulus (Fis), which participates in a variety of cellular functions, accelerate as the concentration of solution-phase proteins increases [7–12], suggesting that cellular concentration level of a TF could operate as a regulatory feedback mechanism. The single-molecule tracking experiments in living cells with relatively low-abundance metalloregulatory TFs such as CueR and ZuR have provided some evidence in this direction [12, 13]. However, whether such a concentration-dependent mechanism can be functional in cellular conditions for structural TFs such as Fis, which has the ability to significantly alter the chromosome structure in a concentration-dependent manner while undergoing large concentration fluctuations, has been elusive.

Fis is one of the most extensively studied dual-purpose *Escherichia coli* (*E. coli*) nucleoid binding proteins [14–16], and it functions both as a TF and a structural protein [17–19]. Fis *in vivo* has growth-dependent concentration levels [20], and under nutrient-rich conditions, it can increase its cellular concentration level from less than a hundred to 60.000 copies per cell and returns its initial limits by the end of the exponential phase [16, 20]. During this concentration rise and fall, Fis binds to DNA sequence specifically and participates in the regulation of more than 200 genes (either as an activator or repressor) necessary for growth, replication, and energy metabolism [20–23]. Fis can also bind to DNA in a nonspecific manner with a lower affinity than that of specific binding [24, 25]. Through bending the DNA or bridging of remote regions of the chromosome, Fis alters the nucleoid structure [26] and stabilizes DNA loops *in vitro* [27]. Considering a possible correlation between the diverse functions of Fis and its large concentration fluctuations in physiological conditions, Fis emerges as an ideal candidate to study the generic effects of TF-concentration variations on protein unbinding kinetics and chromosome condensation.

Fis is also one of the first TFs identified to undergo a concentration-dependent unbinding via a mechanism referred to as facilitated dissociation (FD) from its nonspecific and specific binding sites [7–9]. In the micromechanical assays, initially DNA-bound GFP-Fis exchanged with unbound Fis molecules in solution [9]. While the dissociation of Fis took as long as several hours when there were no competing proteins in the solution, the addition of binding competitors to the solution even at several hundred nanomolars reduced average dissociation

times from hours to minutes. The FD of Fis also occurs with isolated bacterial chromosomes [8]. More recently, *in vitro* single-molecule fluorescence studies with surface-immobilized 22-bp binding sites confirmed that FD can occur at a single binding site level [7]. The computational models also supported these observations [11, 12]. Similar dissociation patterns occur when competing Fis was replaced by competing nucleic acid segments [28], in accord with chromosome compaction-dependent dissociation of several metalloregulator TFs [12]. The underlying mechanism of FD is attributed to the multivalent binding nature of these proteins [9, 10]. The multivalency is proposed to allow microscopically dissociated states, in which the protein can expose the binding site temporarily for the invasion of binding competitors from solution [29, 30]. This effect increases as the concentration of competitors in solution increases [7, 9].

Several pioneering particle-tracking experiments with the metalloregulatory TFs provide evidence that FD occurs in live cells [12, 13]. However, FD for Fis has only been shown *in vitro* for proteins unbinding from physically restrained binding sites (i.e., from either sparsely surface-grafted DNA binding sites or extended DNA/chains and chromosomes) [7–9]. Nevertheless, whether FD can occur for Fis in the confinement of the bacterial volume with the same efficiency (i.e., when binding sites are free to diffuse along with the DNA polymer, whose conformation can be altered by Fis) is not clear. Indeed, Fis already exhibited a chromosome condensation activity via the formation of stable Fis-DNA multiprotein complexes at the millimolar-concentration levels [27], suggesting that elevated concentration levels *in vivo* could cause two opposing effects on the unbinding kinetics of Fis.

In this study, we use large-scale molecular dynamics (MD) simulations of a coarse-grained model of *E. coli* bacterium to reveal the potential interplay between variations in Fis concentrations, off-rates, and Fis-related chromosome organization. Such MD simulation have been actively used to study the large-scale long time behaviour of genome [31–33]. In our model, a circular DNA polymers ($\sim 10^5$ bp) are confined by rigid concentric shells. Unlike the previous studies on bacterial chromosome organization [33, 34], a state-of-the-art coarse-grained model of Fis recapitulating the multivalent binding nature of the protein can dynamically interact with the DNA polymer both specifically and non-specifically. This setup allows us to track a large number of Fis molecules simultaneously and monitor the effect of Fis concentration on chromosome structure and unbinding dynamics. Interrogation of various Fis concentrations and binding affinities reveal that FD could occur in the physical confinement of bacterial volume, particularly when the chromosome is of loose structure. At a few millimolar Fis concentrations, specific binding sites of Fis are brought together by protein clusters, and these clusters anchor multiscale loop-like structures. At protein concentrations corresponding to cellular levels of Fis at the early exponential phase, chromosomal compaction significantly slows down the off-rates (i.e., longer residence times). Fis dimers assemble into well-ordered protein-DNA arrays that juxtapose DNA segments into doughnut-shaped structures. At the limit of several hundred millimolars of Fis, Fis completely condenses the chromosomes into a protein-dense globular structure. Finally, we use the available DNA microarray data from the literature and discuss our results in the context of transcriptional diversity of Fis in nutrient-rich conditions.

II. MATERIALS AND METHODS

A. Simulation Model

In our MD simulations, a circular DNA molecule and proteins are modelled using the coarse-grained Kremer-Grest (KG) bead-spring chains in implicit solvent [35, 36]. The nucleic acid chain is a smaller version of the full-size *E. coli* genome with 1.2×10^5 base pairs (bp), which is modelled with $N = 12000$ KG beads with each bead representing ~ 10 bp. The circular DNA chain and proteins are confined by a rigid concentric cylinder with an aspect ratio of 3 (Figure 1A). The caps of the cylinders are built as semi-spheres. The volume of the confinement is adjusted in accordance with the nucleic acid concentration of *E. coli*, which corresponds to a DNA volume fraction of $\sim 1\%$.

The simulation systems consist of two types of proteins: initially DNA-bound and free proteins (Figure 1B). Initially, bound proteins are positioned near promoter regions (red beads represent the binding sites in Figure 1A-C) that are spaced evenly along the DNA polymer. Given the smaller size of our model genome, the number of binding sites is chosen as $n_0 = 120$, which is lower than the consensus sequences determined [37] but high enough to perform statistical analyses of unbinding kinetics [38]. To monitor the concentration-dependent dissociation, a prescribed concentration of initially free proteins, c_{f}, are added at random positions in the simulation boxes in addition to the $n_0 = 120$ initially bound proteins. The total protein concentration in cells ranges between 12 μM (only DNA-bound proteins) and 212 μM, which correspond to $n_0 = 120$ and $n_0 = 2225$ protein copies per cell, respectively.

DNA polymer, proteins, and the confinement boundary are composed of identical beads of size $b = 1\sigma$, where σ is the unit length in the MD simulations. The steric interactions between these beads are modelled by a truncated and shifted Lennard-Jones (LJ) potential, also known as WCA,

$$V^{\mathrm{LJ}}(r) = \begin{cases} 4u\left[(\sigma/r)^{12} - (\sigma/r)^6 + v_s\right] & r \le r_c \\ 0 & r > r_c. \end{cases} \quad (1)$$

The cut-off distance $r_c = 2^{1/6}\,\sigma$, the shift factor $v_s = 1/4$, and the interaction strength $u = 1\ k_{\mathrm{B}}T$ are chosen

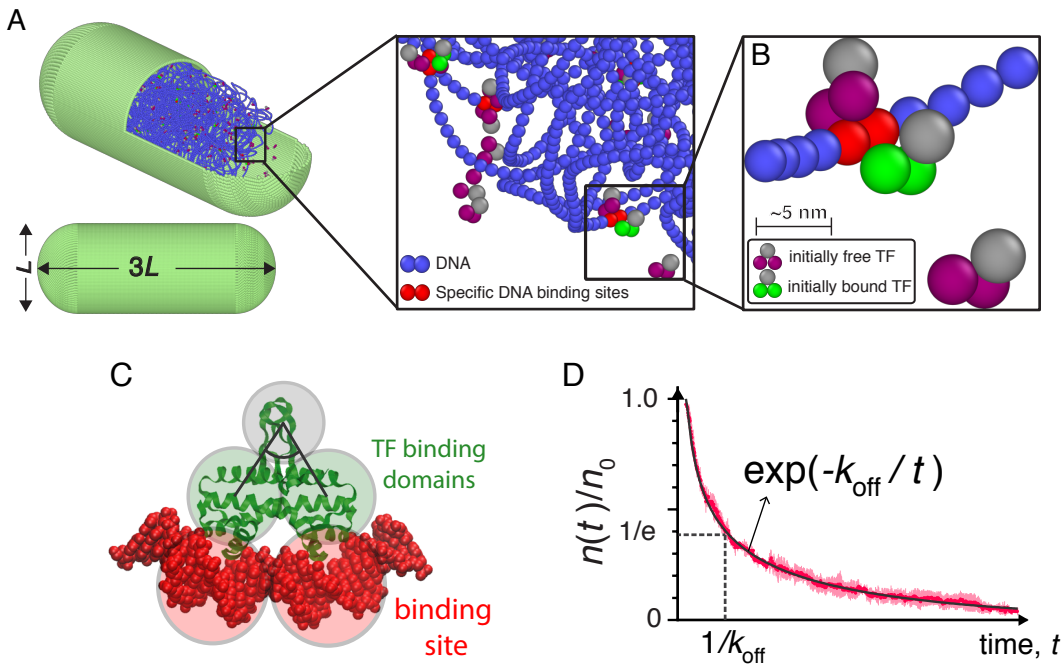

FIG. 1. The schematics of MD simulation model. A) The bacterial DNA polymer (blue and red beads) is confined inside a rigid concentric shell (light green beads) together with initially (i.e., at $t = 0$) bound and free TF proteins. B) Closer look into a single specific binding site (red beads) surrounded by nonspecific sites (blue beads), with which bound and free dimeric Fis TF proteins can dynamically bind to and unbind from. C) Schematics of the coarse-grained dimeric model of Fis, where two binding domains (green beads) are joined by a hinge bead (grey), can interact with the whole DNA chain. D) Extraction of the off-rate, $k_{\rm off}$, from the time-dependent decay of the normalized number fraction of DNA-bound proteins (i.e., survival fraction), $n(t)/n_0$ (see Eq. 5).

to obtain good solvent conditions (i.e., a repulsive interaction) unless otherwise noted. Here, $k_{\rm B}$ is the Boltzmann constant, and T is the absolute temperature. For the attractive interactions between DNA and proteins, we set $r_c = 2.5\ \sigma$ and $v_s = 0$. The interaction strength value is set to $u \gg 1$ to model nonspecific and specific interactions (see below for details). There is no net attraction between the beads of the proteins. The bonding between the adjacent beads of the DNA chain or proteins is taken care of by a nonlinear FENE potential

$$V^{\rm Bond}(r) = -0.5kr_0^2 \ln\left[1-(r/r_0)^2\right], \qquad (2)$$

where the default value of the bond stiffness is $k = 30\ k_{\rm B}T/\sigma^2$. In Eq. 2, the distance between adjacent beads is $r = |\mathbf{r}|$, and the maximum bond length is $r_0 = 1.5\ \sigma$ [35].

A harmonic bending potential is introduced to model the semi-flexible nature of the DNA as

$$V^{\rm Bend}(\Theta) = k_\Theta\left(\Theta-\Theta_0\right)^2, \qquad (3)$$

where the potential strength is $k_\Theta = 15k_{\rm B}T/rad^2$, Θ is the angle formed by three adjacent beads, and Θ_0 is the reference angle and is $\Theta_0 = \pi$ is for the DNA chain. These parameters provide an average persistence length of ∼15 beads [39], which is in accord with the persistence length of naked double-stranded DNA (i.e., ∼150 bp ∼ 50 nm).

All MD simulations are run with LAMMPS MD package [40] at constant volume V and reduced temperature $T_{\rm r} = 1.0$. In the preparation of the setups, each DNA polymer is prepared as a perfect circle of N beads and is larger than the dimensions of the cellular confinement. In order to fit the polymer within the designated volume, the polymer is collapsed by assigning temporary self-attraction energy of 17 $k_{\rm B}T$ between all chain beads. Upon transferring the collapsed polymer inside the cylinders, this attraction is reversed to the default values, and then, the polymer is allowed to relax for $> 2\times10^4$ MD steps. Then, the initially bound proteins are placed on the positions of the respective binding sites. To check if the relaxation of the long polymers has any effect on the results, a shorter chain with $N = 2400$ is tested, but no quantitative difference in unbinding kinetics is observed (Supplementary Figure 1). The data production runs are carried out for $10^6 - 10^9$ MD steps depending on the binding strength and protein concentration. During the simulations, DNA stays within the cellular volume, and occasionally a few proteins (among hundreds) leave the cylinder. The simulations are run with a time step of $\Delta t = 0.005\ \tau$, where the unit time scale in the simulations is τ, which is roughly the self-diffusion time of a single bead in dilute solution. The monomeric LJ mass

is $m = 1$ for all beads. The temperature is kept constant by a Langevin thermostat with a thermostat coefficient $\gamma = 0.5\ \tau^{-1}$. The volume of the total simulation box is set to $L_x \times L_y \times L_z = 184 \times 64 \times 64\ \sigma^3$. Periodic boundary conditions are used in all directions.

B. Cherry model for dimeric Fis TF Protein

Previous MD simulations used a two-bead model for simulating Fis protein [7, 29, 38]. Although the two-bead model was sufficient to simulate multivalency, there is no energy penalty for configurational changes of the protein [41]. Thus, we introduce a simplistic three-bead coarse-grained model, in which binding domains of dimeric TF are joined by a third hinge bead (Figure 1C). This hinge (grey bead in Figure 1A-C) does not interact with DNA. In order to main the average "cherry" shape of the dimeric protein, a harmonic potential with a reference angle of $\Theta_0 = 50°$ is set between the three beads with $k_\Theta = 12 k_{\mathrm{B}} T / rad^2$ in Eq. 3.

C. Estimation of relative strengths of non/specific protein-DNA interactions

In our model, we choose the specific binding energies ranging between 7-20$k_{\mathrm{B}}T$ (i.e., 5-13 kcal/mol in more familiar units of energy), which are close as values estimated via theoretical calculations [42], experiments of Fis-assisted loop formation [27], and potential-mean force simulations [41]. However, Fis is known to bind to DNA nonspecifically as well but with a lower binding affinity [24, 25]. In order to estimate the relative difference in binding energies between the specific (SP) and nonspecific (NS) interactions, we use the dissociation constants reported in the literature According, K_{d} values for two cases differ roughly a factor of ~ 1000 [23]. We use the expression

$$K_{\mathrm{d}}^{\mathrm{SP}} / K_{\mathrm{d}}^{\mathrm{NS}} \sim \ln\left(\Delta u / k_{\mathrm{B}} T\right), \tag{4}$$

to estimate the difference between the interaction strengths of non/specific interactions as $\Delta u \sim 7 k_{\mathrm{B}} T$. Throughout our simulations, we maintain this difference while varying the strength of the specific interactions. Note that in Eq. 4, we assume that entropic contributions to the non/specific unbinding free energies are similar.

D. Calculation of off-rates

To monitor the unbinding kinetics, the number of proteins remaining bound on their binding sites, $n(t)$, is monitored as a function of the simulation time, t. If any bound protein leaves out of a spherical volume with a radius $R_c = 2.5\sigma$, centred around the centre of mass of the binding site (red beads in Figure 1), the protein is tagged as dissociated. The distance R_c roughly corresponds to the self-diffusion distance of the protein. If a dissociated protein re-binds to DNA, it is not counted as bound. To determine the off-rates both in the absence and presence of unbound proteins, the survival fraction data is fit by a single exponential

$$n(t) = n_0 \exp(-k_{\mathrm{off}} t), \tag{5}$$

where k_{off} is the off-rate with the units of inverse time. A representative decay curve is shown in Figure 1D. Error bars are calculated by averaging the results of three independent runs. In the fitting procedures, a weight function inversely proportional to the square of the data point is used. Error bars are not shown if they are smaller than the size of the corresponding data point. Python 3.7 or higher, with the extensive use of NumPy package [43], is used for data analysis of all the resulting simulation data (code available sup. data). VMD and OVITO are used for the visualizations and acquiring the snapshots of the system [44, 45].

III. RESULTS

A. The dissociation of DNA-bound proteins depends on the unbound protein concentration and binding energy

In order to investigate whether FD can occur in the confinement of a prokaryotic cell, and when binding sites are located along the diffusing DNA polymer, we follow a methodology similar to that in a previous *in vitro* single-molecule study [7]. Accordingly, we prepare our systems such that at the beginning of a simulation (i.e., $t = 0$), each specific $\sim$ 20-bp-long binding site, which is around 1000 bp apart from the nearest neighbouring binding sites, is occupied by a single protein (Figure 1A-C). In addition to the initially DNA-bound TF proteins, prescribed concentrations of unbound proteins are added at random positions in the cellular volume. As time progresses in the simulations, the n_0 DNA-bound proteins dissociate into the cellular volume from their binding sites, and the number of DNA-bound proteins decreases (i.e., $n(t) < n_0$ at $t > 0$). The effect of FD is probed by monitoring the time-dependent decay of the survival fraction of bound proteins, $n(t)/n_0$, for various TF concentrations (Figure 1D).

Figure 2 shows the survival fraction of DNA-bound proteins as a function time for various binding energies and initially unbound Fis concentrations. In the case of spontaneous dissociation (SD), for which bound TFs to drop off their binding sites in the absence of unbound Fis in the bacterial volume, the dissociation of DNA-protein from their DNA-binding sites is significantly slow (up triangles in Figure 2A,B) as compared to the cases, in which there are initially free proteins. As the Fis concentration increases, the bound Fis molecules leave their

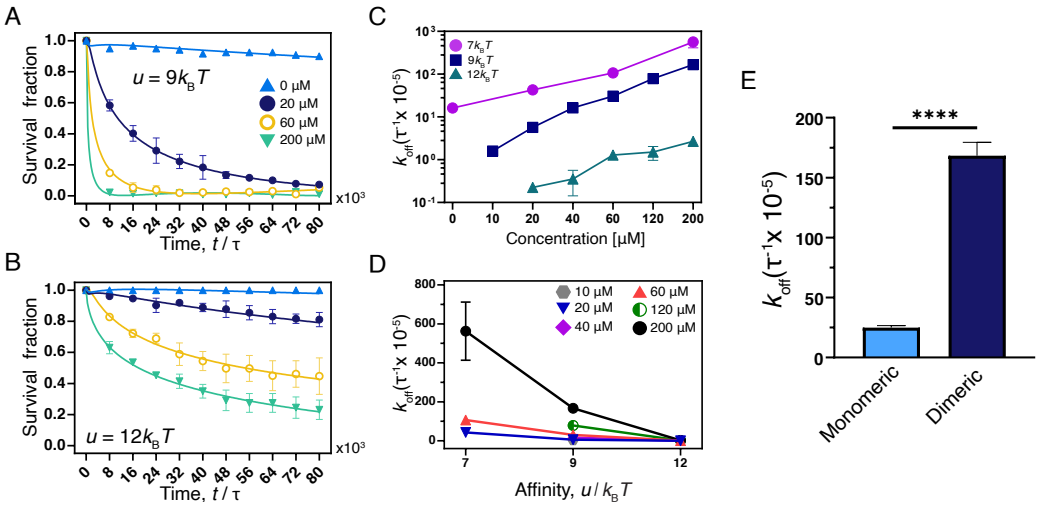

FIG. 2. The evidence of FD in the model cellular confinement. A, B) Survival fractions of bound transcription factors for initially unbound Fis concentrations of 0, 20, 60, 200 μM for various interaction energies between specific DNA sites and Fis. Nonspecific interaction strength is $\Delta u = 7k_{\rm B}T$ lower than that of specific interactions for each case. The solid curves are the exponential fits (Eq. 5). C) The off-rates, $k_{\rm off}$, extracted from the survival-fraction data as a function of unbound Fis concentration and D) as a function of the strength of specific interactions between DNA and protein. The data points are joined to guide the eye. E) The comparison of the off-rates obtained from the separate simulations with monomeric and dimeric Fis models in the presence of initially 200 μM unbound Fis with corresponding valency. In both cases, Fis-DNA binding energy is $u = 9k_{\rm B}T$

binding sites more rapidly (Figure 2A,B). For instance, at 60 μM of Fis and for specific binding energy below $u = 10k_{\rm B}T$, almost all initially DNA-bound molecules leave their specific binding sites after several ten thousands of simulation steps (open circles in Figure 2A).

We observe similar dissociation patterns for DNA-Fis binding energies above $u = 10k_{\rm B}T$; however, the dissociation of DNA-bound proteins significantly slows down, particularly in the absence of free Fis molecules in the cell (i.e., SD in Figure 2B). We estimate that in the SD case, the decay to the half values of the survival fraction for binding energies $u > 10k_{\rm B}T$ would require 1000 times longer simulations, which are not feasible computationally but are at the same time consistent with *in vitro* hours-long dissociation times of Fis [7–9].

B. Facilitated dissociation of DNA-bound proteins can occur in the cellular confinement

The FD phenomenon's main hallmark is the acceleration of off-rates of DNA-bound proteins as the concentration of binding competitor proteins in solution is increased [7, 9, 10, 29]. We extracted the off-rates from the survival-fraction data from Figure 2(see Methods section). The decay data can be fitted by single exponential functions, which allow the extraction of the off-rates via Eq. 5. When the off-rates are plotted against the unbound TF concentration, a consistent increase with increasing Fis concentration is observed regardless of binding affinity (Figure 2C). This indicates that an FD-like mechanism contributes to the rapid dissociation of DNA-bound TFs. Over a concentration range of $0 - 200$ μM, the off-rates exhibit at least a 10-fold increase for binding energies $u < 10k_{\rm B}T$(Figure 2C). As binding energy is increased, the extraction of the off-rates is rather limited by slow dissociation of the initially-DNA bound proteins, particularly at low Fis concentrations. Nevertheless, the difference between the off-rates of SD (i.e., initial Fis concentration is zero) and FD (at the maximum concentration 200 μM) demonstrates the drastic effect of solvated proteins on the unbinding kinetics.

In general, the DNA-protein binding energy determines how strongly the concentration increase of unbound proteins affects the dissociation behaviour (Figure 2D). For instance, if we compare the SD (no unbound Fis) and the FD with 20 μM of unbound Fis in Figure 2A and B for two different binding energies, the low-affinity case (i.e., $u = 9k_{\rm B}T$) is affected by the presence of unbound proteins more strongly as compared to the case where the protein binds tightly to DNA (i.e., $u = 12k_{\rm B}T$). This affinity-dependent behaviour is consistent with the previous simulation studies [29, 38, 46] and theoretical predictions [42], suggesting that low-affinity proteins can be affected from concentration variations more drastically. This behaviour is also in accord with the SD experiments on a smaller yeast TF protein, NHP6A, which binds to DNA with a lower affinity than Fis, but its FD response is at least a factor of two stronger under the equivalent concentration changes [7].

Overall, our MD simulations show that FD indeed could be functional when binding sites are distributed

along the self-avoiding DNA in the cellular confinement. However, as we will discuss in the following sections, Fis can condense the chromosome by bringing distant DNA binding sites together, and thus, it can also alter its dissociation rates via chromosome compaction. In the following sections, we will discuss how protein concentration and binding affinity affect the chromosome architecture and which, in turn, unbinding kinetics.

C. A monovalent Fis model does not exhibit facilitated-dissociation behaviour

The concentration-dependent off-rates occurring for various protein species is explained by the multiple-binding site mechanism of the DNA-bound proteins [7, 29, 30]; The weak molecular interactions transiently anchoring the protein to the DNA binding site can partially break and expose the binding site for solvated proteins. In our dimeric Fis model, this multivalency is achieved by the two independent binding domains (Figure 1C). We reasoned that replacing the dimeric Fis with a monovalent protein model (i.e., the protein is composed of a single bead, and thus, can be either DNA-bound or free states) should eliminate any multivalency-driven effect such as FD. Figure 2E, we compare the off-rate obtained from the simulation with the monovalent Fis model to that from the dimeric Fis. Although both dimeric and monovalent Fis bind to the DNA with the same binding energy (i.e., $u = 9k_{\mathrm{B}}T$), the dimeric Fis dissociates more rapidly at an identical concentration of unbound (i.e., 200 μM) (Figure 2E). This behaviour suggests that the phenomenon that we observe in our simulations is indeed FD, and it diminishes if the multivalency of the protein is removed.

D. Simulations confirm that Fis alters the 3D chromosome structure in a concentration and affinity-dependent manner

in vitro experiments demonstrated that Fis can increase the branching of isolated bacterial DNA [26] and also compact isolated chromosomes by densely coating the DNA in a concentration-dependent manner [27]. Our simulations validate the effects of concentration variation of Fis on the chromosome compaction qualitatively (Figure 3). In order to characterize the chromosome compaction, we calculate the radius of gyration of the circular DNA polymer, R_{g} (see Methods section). In the absence of proteins, the size of the chromosome is determined by the dimensions of the cellular confinement (i.e., $R_{\mathrm{g}} \sim 50\sigma$). As the TF concentration and binding affinity of the protein are varied, the structure of the chromosome changes between a globular-polymer and a swollen-polymer states as a result of the protein-DNA interactions (Figure 3).

At the unbound Fis concentrations below 20 μM (roughly 1 TF copy per 400 bp in the entire system), we observe protein-dense nodes that form via bridging of multiple specific binding sites, regardless of the strength of the binding energy (Figure 3A,B, the columns at the very left). In the equilibrium configurations, all Fis molecules are clustered around these nodes. Since, in our model, neither Fis nor DNA bears attractive interactions for themselves, such formations are only possible if each protein is shared by multiple binding sites. At these concentration levels, the protein-rich nodes are unable to compact the DNA, and the chromosome pervades a considerable portion of the cellular interior (Figure 3A and B, left column). This open chromosome structure is in accord with the simulations based on the Hi-C contact maps of Fis deficient cells [47].

If the concentration of Fis is increased above 20 μM, the chromosome architecture becomes highly sensitive to the DNA-protein binding energy in our simulations (Figure 3C). At binding energies below $u \sim 10k_{\mathrm{B}}T$, the radius of gyration of the chromosome structure has almost no visible dependence on the Fis levels (Figure 3D). Moreover, although Fis molecules can bind to the DNA either specifically or nonspecifically, we observe a considerable amount of Fis (e.g., 40% for an initial Fis levels of 200 μM) freely diffusing throughout the relatively open chromosome structure (Figure 3A, right panel). When we turn our attention to the monovalent Fis model, more Fis (i.e., on average 60 %) are found bound to DNA (Figure 3E). This behaviour suggests that high turnover rates due to FD of Fis from low-affinity nonspecific sites lower the genome occupation of the proteins.

In contrast to the binding energies below $u < 10k_{\mathrm{B}}T$, the binding energies above $u = 10k_{\mathrm{B}}T$ significantly decreases the characteristics size of the chromosomes in a concentration-dependent manner (Figure 3C,D). Further, when Fis interacts with the DNA polymer with the binding affinities $u > 10k_{\mathrm{B}}T$, almost all Fis molecules are in the DNA-bound state, regardless of the cellular Fis concentration (Figure 3B). A visual investigation reveals that as the Fis concentration is increased, the DNA-bound Fis results in larger protein clusters as compared to the lower affinity cases (Figure 3B). However, the population of the clusters decreases with increasing Fis levels, suggesting a relation between the Fis levels and co-localization of high-affinity binding sites by Fis. These proteins clusters anchor protein-free DNA segments in various sizes, which have apparent loop-like conformations (Figure 3B, second column). Noteworthy, the configuration of these DNA segments resemble electric field lines emanating from oppositely charged particles.

At Fis concentration of ~ 60 μM, which corresponds to the peak concentration levels during the growth cycle (i.e., transition from lag phase to the exponential phase [16, 20], the protein clusters seem to form higher-order protein-DNA complexes. Such protein-dense complexes, where Fis coats the DNA substrate densely were reported previously at several micromolars [27]. In addition, our simulations show that these complexes can

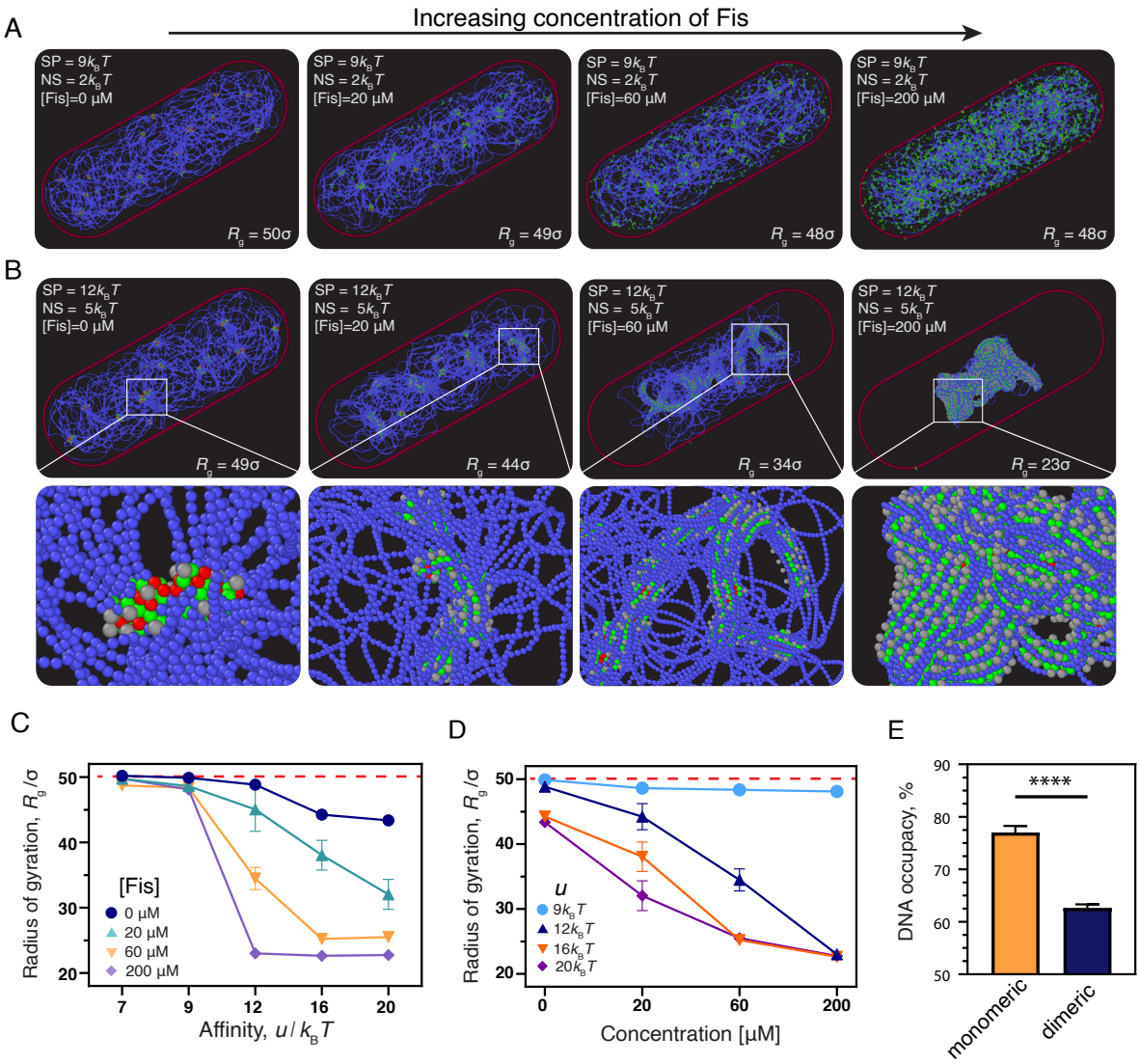

FIG. 3. The role of the Fis concentration and the binding affinity in the chromosomal compaction. A, B) Representative snapshots of chromosomal structures for the initially unbound Fis concentrations of 0, 20, 60, and 200 μM (left-to-right) for specific (SP) binding energies of $u = 9, 12k_{\rm B}T$. The blue and red beads correspond to nonspecific and specific DNA binding sites, respectively. The green and grey beads correspond to Fis binding and hinge domains, respectively. Initially bound and unbound Fis are both marked by the same colors in the snapshots. The beads of the cell boundary are indicated by magenta. C) The calculated values of radius of gyration, $R_{\rm g}$, as a function of Fis concentration for various binding energies. D) $R_{\rm g}$ as a function binding affinities at various Fis concentrations. The horizontal dashed lines in C and D are the $R_{\rm g}$ values of the DNA polymer in the absence of proteins. In C and D, the data points are joined to guide the eye. E) DNA occupancy of monomeric and dimeric Fis models in the presence of initially 200 μM unbound Fis with identical valency. In both cases, Fis-DNA binding energy is $u = 9k_{\rm B}T$

be juxtaposed by Fis interacting nonspecifically with Fis to form large-scale doughnut-shaped protein-DNA structures (the third column of Figure 3B). These structures are stabilized by relatively well-ordered protein-DNA complexes. The formation of multiprotein complexes expanding beyond the clusters about the specific sites results in a highly condensed chromosome structures with values of R_g much smaller than the cases with lower Fis levels (Figure 3C,D).

In order to observe the limiting regimes of chromosome structure, we increase the Fis levels to an excess level of 200 μM, which is more than physiological concentrations. In principle, such high Fis concentrations are not possible *in vivo*, however, inhomogeneous distribution of proteins throughout the cell may cause such over-condensation at smaller genomic scales, which can sterically reduce the accessibility by transcription machinery. At this Fis levels, the entire chromosome structure is completely con-

densed to a globular state (Figure 3B, the frame on the right side). This collapsed regime is robust and occurs for any binding affinity $u > 10k_{\mathrm{B}}T$ (purple diamonds in Figure 3C). The surface of the collapsed structure is covered by well-ordered protein arrays. Notably, the size of the collapsed chromosomes corresponds to the smallest possible size of the DNA polymer in our simulations, which is defined as the polymer size in poor solvent conditions, $R_g \sim N^{1/3}\sigma \sim 23\sigma$, where $N = 12000$ (Figure 3C,D).

In summary, our MD simulations suggest that cellular protein levels of the structural TF Fis can compact the chromosome starting from the genomic regions containing relatively high-affinity binding sites. The binding sites with low affinity allow high protein turnover rates (short residence times), however, they do not contribute to the condensation of the chromosome.

E. The off-rate is high if the chromosome is loose and slows down as chromosome condenses

Now we return to our discussion on TF unbinding kinetics. The aforementioned conformation changes of chromosomes imposed by variation in Fis concentrations and binding affinity have drastic effects on the off-rates (Figure 4). If we plot the off-rates from Figure 2C as a function of the corresponding chromosome size, R_{g}, we find that the off-rates has almost no dependence on R_{g} for binding affinities $u < 10k_{\mathrm{B}}T$ (Figure 3A, gray shaded area; see Supplementary Figure 4 for the complete data set). Since, in this regime, the size of a chromosome has almost no dependence on the TF concentration (Figure 3A,C), the calculated off-rates do not have any apparent dependence on chromosome-compaction levels and are mainly governed by the binding affinity and concentration of TFs (Figure 4A).

Contrarily, at the binding energies of $u > 10k_{\mathrm{B}}T$, for which Fis molecules tightly bind to the DNA both at specific and nonspecific locations and lead to a gradual compaction of the chromosome structure with increasing TF concentrations (Figure 3B-D), the concentration-dependent compaction significantly reduces the off-rates (Figure 4A). Notably, as R_g is decreased by a factor of ~ 2, the off-rates decrease more than a factor of 10.

Our simulations suggest binding affinity and chromosome-compaction levels cumulatively affect the off-rates. To decouple these two effects, we test a hypothetical situation in which nonspecific interactions between TFs and DNA polymer are set to zero such that Fis can only specifically interact with the DNA. One immediate result of omitting nonspecific interactions is a more loose chromosome structure regardless of binding strength or protein concentrations (Figure 4B). When nonspecific interactions are removed, the chromosome never collapses, confirming the role of nonspecific interaction in the 3d genome organization. Furthermore, since there are not enough binding sites for all the Fis molecules on the DNA, once all the specific binding sites are saturated by Fis, the remaining Fis fills the cellular volume (Figure 4B). This loose chromatin structure allows the interaction between the free Fis and bound Fis molecules, thus, significantly increases the off-rates (Figure 4C,D). Even at the binding strengths, at which no dissociation is observed in the presence of the nonspecific interactions, a substantial amount of dissociation is observed (Figure 2C). For instance, at $u = 20k_{\mathrm{B}}T$, the calculated off-rate at zero unbound Fis accelerates almost three orders of magnitude (Figure 4C), suggesting that the compaction of local DNA structure by nonspecifically interacting structural TFs can drastically increase the residence times.

F. Both lower and higher affinity proteins can replace the DNA-bound proteins via FD

So far in our simulations, the initially DNA-bound and unbound Fis TFs have equal binding affinities towards the DNA. Nevertheless, various Fis mutants can coexist and compete for the same binding site with relatively similar affinities (with $K_d \sim 1$ nm) [23, 48]. For instance, the relative difference in the binding affinities of K94A mutant and wild type Fis is factor of ~ 4 [23], resulting in a relative difference of $\sim 1k_{\mathrm{B}}T$ in the strengths of interactions energies via Eq. 4. Moreover, DNA-bound Fis was shown to exchange with HU molecules from solution in single-molecule experiments, indicating the heterotypic nature of FD [9].

To reveal the competition between DNA-bound and free proteins but with relatively lower/higher affinities, we perform simulation by setting a difference of $\sim 1k_BT$ in the binding strengths of the initially DNA-bound and unbound Fis dimers. For simplicity, we choose the affinity of the DNA-bound Fis as $u = 9k_{\mathrm{B}}T$, for which the chromosome is relatively loose, and the FD does not suffer from chromosome compaction (Figure 3A). Our simulations show that both relatively lower ($u = 8k_{\mathrm{B}}T$) and higher ($u = 10k_{\mathrm{B}}T$) affinity Fis are able to facilitate the dissociation of the DNA-bound Fis efficiently (Figure 5). However, the higher-affinity proteins are more effective in stripping the lower affinity TFs off their binding sites (Figure 5B). This heterotypic behaviour is observed for larger concentration ranges and seems to be more effective as Fis concentrations is increased .

IV. DISCUSSION

A. Concentration-dependent off-rates (residence times) can have regulatory effects on transcription *in vivo*

As the cellular concentration of a TF protein increases, the probability of the protein to find its DNA target site increases linearly with the concentration [49]. As the TF proteins bind to their target genes, up or down-regulation

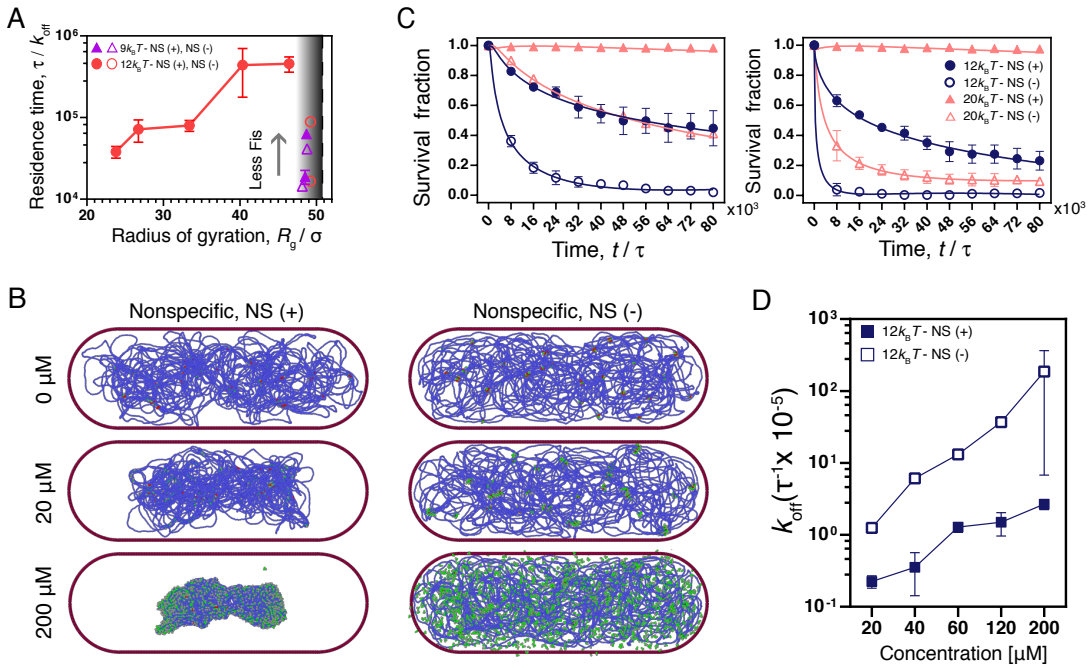

FIG. 4. Chromosomal compaction versus unbinding kinetics with and without nonspecific interactions. A) The inverse of off-rates (i.e., residence times), $1/k_{\rm off}$ as a function of the calculated radius of gyrations, R_g, for various binding affinities and Fis concentrations. B) Representative snapshots of chromosomal structure for initially unbound Fis concentrations of 0, 20, and 200 μM with (NS+) and without nonspecific (NS-) interactions. The specific binding energy (NS) is $u = 20k_{\rm B}T$ in all-cases. The blue and green beads correspond to DNA chain and Fis molecules, respectively. C) The survival fraction of DNA-bound Fis as a function of time for $u = 12, 20k_{\rm B}T$ with and without NS interactions at initially unbound Fis concentrations of 0 and 200 μM. The curves are exponential fits by Eq. 5. D) The calculated off-rates for $u = 12k_{\rm B}T$. in A and E, the data points are joined to guide the eye. In the cases where NS is on (i.e., NS+), nonspecific interaction is $\Delta u = 7k_{\rm B}T$ lower than the corresponding specific binding strength.

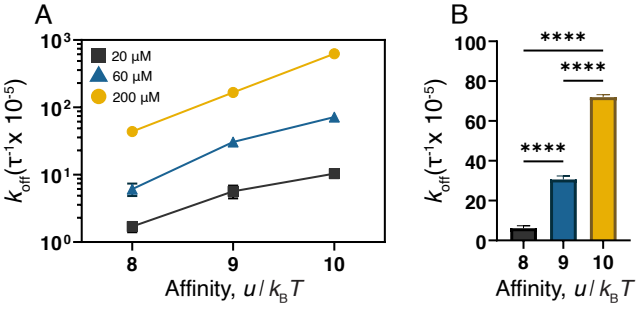

FIG. 5. Heterotypic behavior of FD for Fis. A) The off-rates of Fis, $k_{\rm off}$, that interact with DNA with a specific binding strength of $u = 9k_{\rm B}T$ for various concentration of initially unbound Fis. The binding strengths of the initially unbound proteins are varied between $u = 8 - 10k_{\rm B}T$. B) The off-rates at the Fis concentration of 20 μM for three cases; when the initially unbound proteins have lower, equal, and higher affinity than initially DNA-bound proteins.

of the corresponding genes increases. However, this view implicitly assumes that the concentration only affect the on rates (i.e., binding rates) but have no effect on the off-rates, which is defined as the reciprocal of the residence time of the TF on its binding site. However, a series of single-molecule studies reported a systematic increase in the off-rates of various DNA-binding proteins, from Fis to replication protein A, with increasing concentration of the proteins in solution [11, 50–55]. Our extensive MD simulations, where the DNA-bound proteins are allowed to unbind from their specific binding sites along a self-avoiding circular DNA polymer of a biologically relevant length, thus, mimicking *in vivo* conditions partially, support those results and further suggest that FD can occur even when the binding sites are distributed throughout the cellular volume for a wide range of TF concentrations and protein-DNA binding energies. In accord with our findings, both apo and holo forms of various metal-sensing TFs show concentration-dependent off-rates from their specific binding sites in live *E. coli* cells [12, 13]. Moreover, since Fis can change DNA architecture in a concentration-dependent manner, our results indicate that the high levels of Fis (> 10 μM) can alter the 3d structure for the chromosome, and thus, significantly decrease the off-rates of Fis by trapping them in protein-dense clusters.

The key question to answer is whether the transcription output of a gene depends on the residence time of the

corresponding regulator or not. The competition ChIP experiments on the *Saccharomyces cerevisiae* Rap1 TF showed a direct correlation between the residence time and transcriptional output; While long residence times were coupled to transcriptional activation, the low transcriptional output is correlated with rapid unbinding. [6]. Another *Saccharomyces cerevisiae* TF, Abf1, has also exhibited one order of magnitude variation in the off-rates on different binding sites, each of which is related to a different functionality [5]. More recently, by tuning the number of nucleotide-recognizing repeat domains of transcription activator-like effectors (TALEs), a residence time-dependent decrease in the transcription levels of the glucocorticoid receptor-activated gene SGK1 was observed [4]. Thus, based on those and our results, we can postulate that if the residence time of a TF affects its transcription output, any physiological element modulating the residences time, such as the concentration of binding competitors, can also be a regulatory component. In the cases of structural TFs (i.e., Fis), this modulation intermingled with chromosome structural alterations induced by the protein.

B. A tentative molecular picture for Fis-induced chromosome compaction

The high-resolution contact maps of *E. coli* chromosomes revealed a correlation between the high expression levels and structures that are rich in short-range contacts [56]. Furthermore, several fluorescence studies demonstrated that Fis, along with HN-S and RNA polymerase, can form foci in bacterial cells growing rapidly [57, 58]. Our simulations present a molecular picture for the formation of such potentially transcriptionally active protein-DNA structures by using Fis-DNA interactions as a platform. At Fis concentrations of ~ 1 μM, Fis mainly binds to high-affinity specific sites and manage to bridge multiple binding sites. These protein clusters are spread evenly throughout the relatively open bacterial chromosomes (Figure 3), which is in accord with Hi-c esperiments with Fis defient cells [56]. Multiscale loop-like structures that are poor in high-affinity sites are anchored by these protein clusters, confirming that such high-affinity sites can be functional in organizing DNA [59, 60]. At the Fis levels of ~ 10 μM, which correspond to the protein levels at the early to mid lag phase, Fis forms more populated protein clusters around the high-affinity sites. However, these clusters are fewer in number compared to the lower-Fis conditions, which indicates the coalescence of more specific sites at the protein clusters. Noteworthy, at ~ 1 μM of Fis levels in our equilibrium configurations, the nonspecific DNA segments are mostly protein-free, except those neighbouring the specific sites, confirming the initiation of Fis-DNA complexation from high-affinity sequences [61].

Our simulations suggest that at the peak levels of Fis concentrations, which correspond to the levels at the early exponential phase of the cell growth, Fis localizes both at specific and nonspecific sites since the specific sites are completely saturated. Nonspecific binding of Fis to DNA drives the chromosome compaction further *via* bridging multiple DNA segments into large doughnut-shape structures (Figure 3). These structures juxtapose multiple low mobility DNA-protein complexes, in which DNA is densely coated by Fis [27]. We should underline that these protein-DNA structures emerge despite the absence of a net attraction between the proteins and induce a nonspecific attraction between DNA segments as previously demonstrated for bacterial H-NS [62]. Importantly, if a specific binding site is surrounded by weak affinity binding sites, our results suggest that nonspecific binding cannot collapse the DNA. At the excess Fis levels of ~ 100 μM, the chromosome condenses into a highly compact structure (Figure 3). Almost all proteins are trapped inside or on the surface of this compact structure, and Fis dissociation from the structure is significantly slow as compared to more open configurations.

C. FD and chromosome compaction and the functional diversity of Fis

Despite the high coarse-graining level of our dimeric Fis model, our simulations could offer some clues about the broad functional diversity of Fis as follows: i) During the early stages of the growth, a gradual increase in Fis levels can modulate Fis residence times differently on different target sequences via facilitated dissociation. In turn, FD-induced variations in residence times can lead to different functional outcomes [4–6]. ii) Fis could lead to temporal DNA compaction via protein-dense clusters at the regions containing Fis regulated gene. ii) Depending on the affinity of nonspecific sites surrounding the gene or physical proximity of other specific sites nearby the gene, DNA-compaction levels (and protein clustering) may differ and sterically inhibit RNA polymerase's access to the region in a selective way. iii) As Fis concentration increases, its autoregulation capacity decreases via FD (i.e., it cannot exclude RNA polymerase effectively [20**?**]). Through the lag phase to the early exponential phase, this repressive behaviour pursuits.

To support our view, we compare the time course of Fis protein and transcript levels in nutritional upshift [20]. Since the expression of Fis is significantly regulated at the transcriptional level, protein abundance is expected to be similar to the transcript levels with a time lag of $\sim$10 minutes [20]. Accordingly, when the cellular level of Fis reached halfway through its maximum, the transcript level of Fis was already at its maximum. Consistently, the available DNA microarray expression profiles showed a cumulative upregulation pattern for Fis-regulated genes within the early exponential phase [22]. Once the Fis level attains its maximum at around $\sim$50 μM (i.e., the level, at which we observe high DNA compaction and

dense protein-DNA arrays in our simulations), Fis levels began to decrease [20, 22]. This decrease continued from the early logarithmic phase to the stationary phase. Within this interval, the transcript levels of Fis decreased from its peak level to vanishing values. This decrease could be due to DNA compaction and/or dense-protein clusters that extend the residence times of Fis. Indeed, this mechanism could be a generic mechanism for gene regulation.

In conclusion, our extensive MD simulations suggest that off-rates of a transcription factor unbinding from DNA, its cellular concentration levels, and the structural changes of chromosome resulting from the concentration variations of the protein can be intermingled. Cumulatively, these effects could regulate the protein's biological functionality by modulating its genome-wide residence times. An investigation of genome-wide off-rates of Fis by using dynamic ChIP or other experimental tools [5, 6] would reveal such mechanisms. Finally, beyond prokaryotic cells, the phenomenon that we demonstrate here is very likely to be functional in eukaryotic cell nuclei as well, given that some structural DNA-binding proteins, such as histone proteins, have already showed some evidence of an FD like mechanism [53, 63]

ACKNOWLEDGEMENTS

AE acknowledges J.F. Marko for the discussion on the Fis binding energies. AGA is supported by TUBITAK 2247-C STAR program. This research is supported by TUBITAK 3501 and 2232 (2018/4) with grant numbers 119Z029 and 119C010, respectively.

Data availability

All the Python codes can be accessed at https://github.com/ZaferKosar/FD.git

Conflict of interest statement.

None declared.

[1] Douglas F. Browning and Stephen J. W. Busby. The regulation of bacterial transcription initiation. *Nature Reviews Microbiology*, 2:57–65, January 2004.

[2] Aswin Sai Narain Seshasayee, Karthikeyan Sivaraman, and Nicholas M. Luscombe. *An Overview of Prokaryotic Transcription Factors*, pages 7–23. Springer Netherlands, Dordrecht, 2011.

[3] Matthew Slattery, Tianyin Zhou, Lin Yang, Ana Carolina Dantas Machado, Raluca Gordân, and Remo Rohs. Absence of a simple code: how transcription factors read the genome. *Trends in Biochemical Sciences*, 39(9):381–399, September 2014.

[4] Karen Clauß, Achim P Popp, Lena Schulze, Johannes Hettich, Matthias Reisser, Laura Escoter Torres, N Henriette Uhlenhaut, and J Christof M Gebhardt. DNA residence time is a regulatory factor of transcription repression. *Nucleic Acids Research*, 45(19):11121–11130, August 2017.

[5] Wim J de Jonge, Mariël Brok, Philip Lijnzaad, Patrick Kemmeren, and Frank CP Holstege. Genome-wide off-rates reveal how DNA binding dynamics shape transcription factor function. *Molecular Systems Biology*, 16(10):1405–16, October 2020.

[6] Colin R Lickwar, Florian Mueller, Sean E Hanlon, James G McNally, and Jason D Lieb. Genome-wide protein-DNA binding dynamics suggest a molecular clutch for transcription factor function. *Nature*, 484(7393):1–7, April 2012.

[7] Ramsey I Kamar, Edward J Banigan, Aykut Erbaş, Rebecca D Giuntoli, Monica Olvera de la Cruz, Reid C Johnson, and John F Marko. Facilitated dissociation of transcription factors from single DNA binding sites. *Proceedings of the National Academy of Sciences*, 114(16):E3251–E3257, April 2017.

[8] N Hadizadeh, Reid C Johnson, and J F Marko. Facilitated dissociation of a nucleoid protein from the bacterial chromosome. *Journal of bacteriology*, 2016.

[9] J S Graham, Reid C Johnson, and J F Marko. Concentration-dependent exchange accelerates turnover of proteins bound to double-stranded DNA. *Nucleic Acids Research*, 39(6):2249–2259, March 2011.

[10] Chandra P Joshi, Debashis Panda, Danya J Martell, Nesha May Andoy, Tai-Yen Chen, Ahmed Gaballa, John D Helmann, and Peng Chen. Direct substitution and assisted dissociation pathways for turning off transcription by a MerR-family metalloregulator. *Proceedings of the National Academy of Sciences*, 109(38):15121–15126, September 2012.

[11] Aykut Erbaş and John F Marko. ScienceDirect How do DNA-bound proteins leave their binding sites? The role of facilitated dissociation. *Current Opinion in Chemical Biology*, 53:118–124, October 2019.

[12] Tai-Yen Chen, Ace George Santiago, Won Jung, Łukasz Krzemiński, Feng Yang, Danya J Martell, John D Helmann, and Peng Chen. Concentration- and chromosome-organization-dependent regulator unbinding from DNA for transcription regulation in living cells. *Nature Communications*, 6:7445, July 2015.

[13] Won Jung, Kushal Sengupta, Brian M Wendel, John D Helmann, and Peng Chen. NAR Breakthrough Article Biphasic unbinding of a metalloregulator from DNA for transcription (de)repression in Live Bacteria. pages 1–10, February 2020.

[14] A. Travers, R. Schneider, and G. Muskhelishvili. Dna supercoiling and transcription in escherichia coli: The fis connection. *Biochimie*, 83 2:213–7, 2001.

[15] Martijn S. Luijsterburg, Maarten C. Noom, Gijs J.L. Wuite, and Remus Th. Dame. The architectural role of

nucleoid-associated proteins in the organization of bacterial chromatin: A molecular perspective. *Journal of Structural Biology*, 156(2):262–272, 2006.

[16] Shane C Dillon and Charles J Dorman. Bacterial nucleoid-associated proteins, nucleoid structure and gene expression. *Nature Reviews Microbiology*, 8(3):1–11, February 2010.

[17] Charles J. Dorman and Kelly A. Kane. DNA bridging and antibridging: a role for bacterial nucleoid-associated proteins in regulating the expression of laterally acquired genes. *FEMS Microbiology Reviews*, 33(3):587–592, 05 2009.

[18] Christina Kahramanoglou, Aswin S. N. Seshasayee, Ana I. Prieto, David Ibberson, Sabine Schmidt, Jurgen Zimmermann, Vladimir Benes, Gillian M. Fraser, and Nicholas M. Luscombe. Direct and indirect effects of H-NS and Fis on global gene expression control in Escherichia coli. *Nucleic Acids Research*, 39(6):2073–2091, 11 2010.

[19] Helge Auner, Malcolm Buckle, Annette Deufel, Tamara Kutateladze, Linda Lazarus, Ramesh Mavathur, Georgi Muskhelishvili, Iain Pemberton, Robert Schneider, and Andrew Travers. Mechanism of transcriptional activation by FIS: Role of core promoter structure and DNA topology. *Journal of Molecular Biology*, 331(2):331–344, August 2003.

[20] C A Ball, R Osuna, K C Ferguson, and Reid C Johnson. Dramatic changes in Fis levels upon nutrient upshift in Escherichia coli. *Journal of bacteriology*, 174(24):8043–8056, December 1992.

[21] W Ross, J F Thompson, J T Newlands, and R L Gourse. E.coli Fis protein activates ribosomal RNA transcription in vitro and in vivo. *The EMBO Journal*, 9(11):3733–3742, 1990.

[22] Meranda D Bradley, Michael B Beach, A P Jason de Koning, Timothy S Pratt, and Robert Osuna. Effects of Fis on Escherichia coli gene expression during different growth stages. *Microbiology*, 153(9):2922–2940, September 2007.

[23] Leah S Feldman-Cohen, Yongping Shao, Derrick Meinhold, Charmi Miller, Wilfredo Colón, and Robert Osuna. Common and Variable Contributions of Fis Residues to High-Affinity Binding at Different DNA Sequences. *Journal of bacteriology*, 188(6):2081–2095, March 2006.

[24] David C Grainger, Douglas Hurd, Martin D Goldberg, and Stephen J W Busby. Association of nucleoid proteins with coding and non-coding segments of the Escherichia coli genome. *Nucleic Acids Research*, 34(16):4642–4652, September 2006.

[25] Yongping Shao, Leah S Feldman-Cohen, and Robert Osuna. Functional Characterization of the Escherichia coli Fis–DNA Binding Sequence. *Journal of molecular biology*, 376(3):771–785, February 2008.

[26] R Schneider, R Lurz, G Lüder, C Tolksdorf, A Travers, and G Muskhelishvili. An architectural role of the Escherichia coli chromatin protein FIS in organising DNA. *Nucleic Acids Research*, 29(24):5107–5114, December 2001.

[27] Dunja Skoko, Daniel Yoo, Hua Bai, Bernhard Schnurr, Jie Yan, Sarah M McLeod, John F Marko, and Reid C Johnson. Mechanism of Chromosome Compaction and Looping by the Escherichia coli Nucleoid Protein Fis. *Journal of molecular biology*, 364(4):777–798, December 2006.

[28] Rebecca D Giuntoli, Nora B Linzer, Edward J Banigan, Charles E Sing, Monica Olvera de la Cruz, John S Graham, Reid C Johnson, and John F Marko. DNA-Segment-Facilitated Dissociation of Fis and NHP6A from DNA Detected via Single-Molecule Mechanical Response. *Journal of molecular biology*, 427(19):3123–3136, September 2015.

[29] Charles E Sing, Monica Olvera de la Cruz, and John F Marko. Multiple-binding-site mechanism explains concentration-dependent unbinding rates of DNA-binding proteins. *Nucleic Acids Research*, 42(6):3783–3791, January 2014.

[30] Christoffer Åberg, Karl E Duderstadt, and Antoine M van Oijen. Stability versus exchange: a paradox in DNA replication. *Nucleic Acids Research*, 44(10):4846–4854, June 2016.

[31] Angelo Rosa and Ralf Everaers. Structure and Dynamics of Interphase Chromosomes. *PLoS Computational Biology*, 4(8):e1000153–10, 2008.

[32] Leonid A Mirny. The fractal globule as a model of chromatin architecture in the cell. *Chromosome Research*, 19(1):37–51, 2011.

[33] Suckjoon Jun and Bela Mulder. Entropy-driven spatial organization of highly confined polymers: lessons for the bacterial chromosome. *Proceedings of the National Academy of Sciences of the United States of America*, 103(33):12388–12393, August 2006.

[34] J Dorier and A Stasiak. Modelling of crowded polymers elucidate effects of double-strand breaks in topological domains of bacterial chromosomes. *Nucleic Acids Research*, 41(14):6808–6815, August 2013.

[35] Kurt Kremer and Gary S Grest. Dynamics of entangled linear polymer melts: A molecular-dynamics simulation. *Journal of Chemical Physics*, 92(8):5057–5086, April 1990.

[36] Gary S Grest and Michael Murat. Structure of grafted polymeric brushes in solvents of varying quality: a molecular dynamics study. *Macromolecules*, 26(12):3108–3117, 1993.

[37] Priyanka Gawade, Gaurav Gunjal, Anamika Sharma, and Payel Ghosh. Reconstruction of transcriptional regulatory networks of fis and h-ns in escherichia coli from genome-wide data analysis. *Genomics*, 112(2):1264–1272, 2020.

[38] Aykut Erbaş, Monica Olvera de la Cruz, and John F Marko. Effects of electrostatic interactions on ligand dissociation kinetics. *Physical Review E*, 97(2-1):022405, February 2018.

[39] Livia A Moreira, Guojie Zhang, Franziska Müller, Torsten Stuehn, and Kurt Kremer. Direct Equilibration and Characterization of Polymer Melts for Computer Simulations. *Macromolecular Theory and Simulations*, 24(5):419–431, June 2015.

[40] Steve Plimpton. Fast parallel algorithms for short-range molecular dynamics. *Journal of Computational Physics*, 117(1):1–19, 1995.

[41] Min-Yeh Tsai, Bin Zhang, Weihua Zheng, and Peter G Wolynes. Molecular Mechanism of Facilitated Dissociation of Fis Protein from DNA. *Journal of the American Chemical Society*, October 2016.

[42] S Cocco, J F Marko, and R Monasson. Stochastic Ratchet Mechanisms for Replacement of Proteins Bound to DNA. *Physical Review Letters*, 112(23):238101–5, June 2014.

[43] Charles R. Harris, K. Jarrod Millman, Stfan J. van der Walt, Ralf Gommers, Pauli Virtanen, David Cournapeau, Eric Wieser, Julian Taylor, Sebastian Berg, Nathaniel J. Smith, Robert Kern, Matti Picus, Stephan Hoyer, Marten H. van Kerkwijk, Matthew Brett, Allan Haldane, Jaime Fernndez del Ro, Mark Wiebe, Pearu Peterson, Pierre Grard-Marchant, Kevin Sheppard, Tyler Reddy, Warren Weckesser, Hameer Abbasi, Christoph Gohlke, and Travis E. Oliphant. Array programming with NumPy. *Nature*, 585(7825):357–362, 2020.

[44] W Humphrey, A Dalke, and K Schulten. VMD: visual molecular dynamics. *Journal of molecular graphics*, 14(1):33–38, 1996.

[45] Alexander Stukowski. Visualization and analysis of atomistic simulation data with OVITO-the Open Visualization Tool. *MODELLING AND SIMULATION IN MATERIALS SCIENCE AND ENGINEERING*, 18(1), JAN 2010.

[46] Katelyn Dahlke and Charles E Sing. Facilitated Dissociation Kinetics of Dimeric Nucleoid-Associated Proteins Follow a Universal Curve. *Biophysical Journal*, 112(3):543–551, February 2017.

[47] Ankit Gupta, Abdul Wasim, and Jagannath Mondal. Nucleoid associated proteins and their effect on E. coli chromosome. *bioRxiv*, page 2020.11.05.369934, November 2020.

[48] S P Hancock, T Ghane, D Cascio, R Rohs, R Di Felice, and Reid C Johnson. Control of DNA minor groove width and Fis protein binding by the purine 2-amino group. *Nucleic Acids Research*, 41(13):6750–6760, July 2013.

[49] S E Halford and J F Marko. How do site-specific DNA-binding proteins find their targets? *Nucleic Acids Research*, 32(10):3040–3052, June 2004.

[50] S R Joseph, M Palfy, L Hilbert, M Kumar, J Karschau Elife, and 2017. Competition between histone and transcription factor binding regulates the onset of transcription in zebrafish embryos. *elifesciences.org*.

[51] Joseph J Loparo, Arkadiusz W Kulczyk, Charles C Richardson, and Antoine M van Oijen. Simultaneous single-molecule measurements of phage T7 replisome composition and function reveal the mechanism of polymerase exchange. *Proceedings of the National Academy of Sciences*, 108(9):3584–3589, March 2011.

[52] Tina Lebar, Anamp x0017E e Verbiamp x0010D, Ajasja Ljubetiamp x0010D, and Roman Jerala. Polarized displacement by transcription activator-like effectors for regulatory circuits. *Nature Chemical Biology*, pages 1–13, November 2018.

[53] Sinan Kilic, Andreas L Bachmann, Louise C Bryan, and Beat Fierz. Multivalency governs HP1. *Nature Communications*, 6:1–11, 2015.

[54] Y Luo, J A North, S D Rose, and M G Poirier. Nucleosomes accelerate transcription factor dissociation. *Nucleic Acids Research*, 42(5):3017–3027, March 2014.

[55] Bryan Gibb, Ling F Ye, Stephanie C Gergoudis, YoungHo Kwon, Hengyao Niu, Patrick Sung, and Eric C Greene. Concentration-Dependent Exchange of Replication Protein A on Single-Stranded DNA Revealed by Single-Molecule Imaging. *PLOS ONE*, 9(2):e87922, 2014.

[56] Virginia S Lioy, Axel Cournac, Martial Marbouty, Stéphane Duigou, Julien Mozziconacci, Olivier Espéli, Frédéric Boccard, and Romain Koszul. Multiscale Structuring of the E. coli Chromosome by Nucleoid-Associated and Condensin Proteins. *Cell*, 172(4):771–783.e18, February 2018.

[57] T A Azam, S Hiraga, and A Ishihama. Two types of localization of the DNA-binding proteins within the Escherichia coli nucleoid. *Genes to cells : devoted to molecular & cellular mechanisms*, 5(8):613–626, August 2000.

[58] Wenqin Wang, Gene-Wei Li, Chongyi Chen, X Sunney Xie, and Xiaowei Zhuang. Chromosome Organization by a Nucleoid-Associated Protein in Live Bacteria. *Science*, 333(6048):1445–1449, September 2011.

[59] Aleksandre Japaridze, Sylvain Renevey, Patrick Sobetzko, Liubov Stoliar, William Nasser, Giovanni Dietler, and Georgi Muskhelishvili. Spatial organization of DNA sequences directs the assembly of bacterial chromatin by a nucleoid-associated protein. *The Journal of biological chemistry*, 292(18):7607–7618, 2017.

[60] Jian Zhang, Yvonne Zeuner, Alexandra Kleefeld, Gottfried Unden, and Andreas Janshoff. Multiple site-specific binding of Fis protein to Escherichia coli nuoA-N promoter DNA and its impact on DNA topology visualised by means of scanning force microscopy. *Chembiochem : a European journal of chemical biology*, 5(9):1286–1289, 2004.

[61] M Bétermier, D J Galas, and M Chandler. Interaction of Fis protein with DNA: bending and specificity of binding. *Biochimie*, 76(10-11):958–967, 1994.

[62] C A Brackley, S Taylor, A Papantonis, P R Cook, and D Marenduzzo. Nonspecific bridging-induced attraction drives clustering of DNA-binding proteins and genome organization. *Proceedings of the National Academy of Sciences of the United States of America*, 110(38):E3605–E3611, September 2013.

[63] D T Gruszka, S Xie, H Kimura, and H Yardimci. Single-molecule imaging reveals control of parental histone recycling by free histones during DNA replication. *Science advances*, 6(38), 2020.

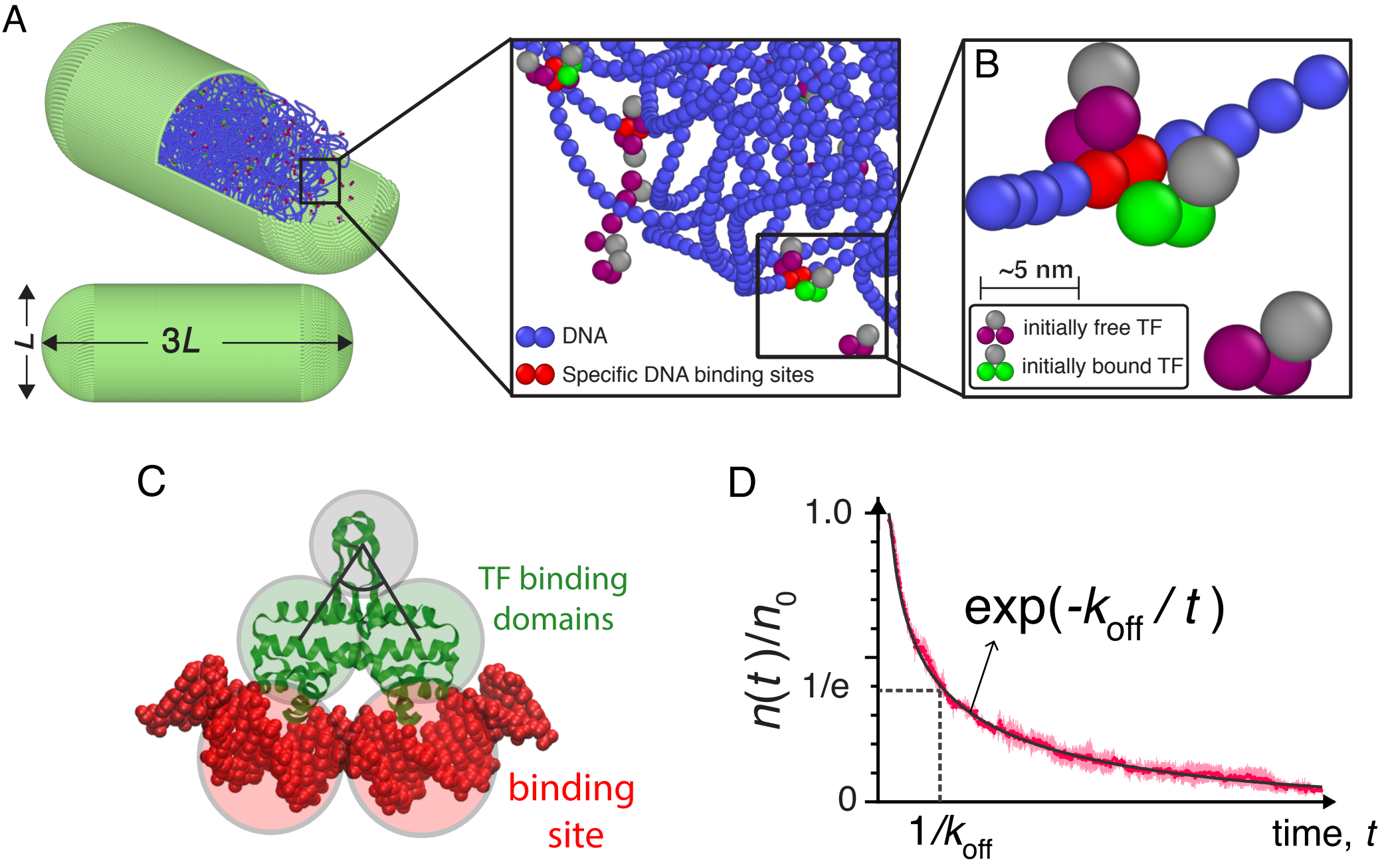
A
L
3L
DNA
Specific DNA binding sites
B
~5 nm
initially free TF
initially bound TF
C
TF binding domains
binding site
D
1.0
1/e
0
n(t)/n0
exp(-koff / t)
1/koff
time, t

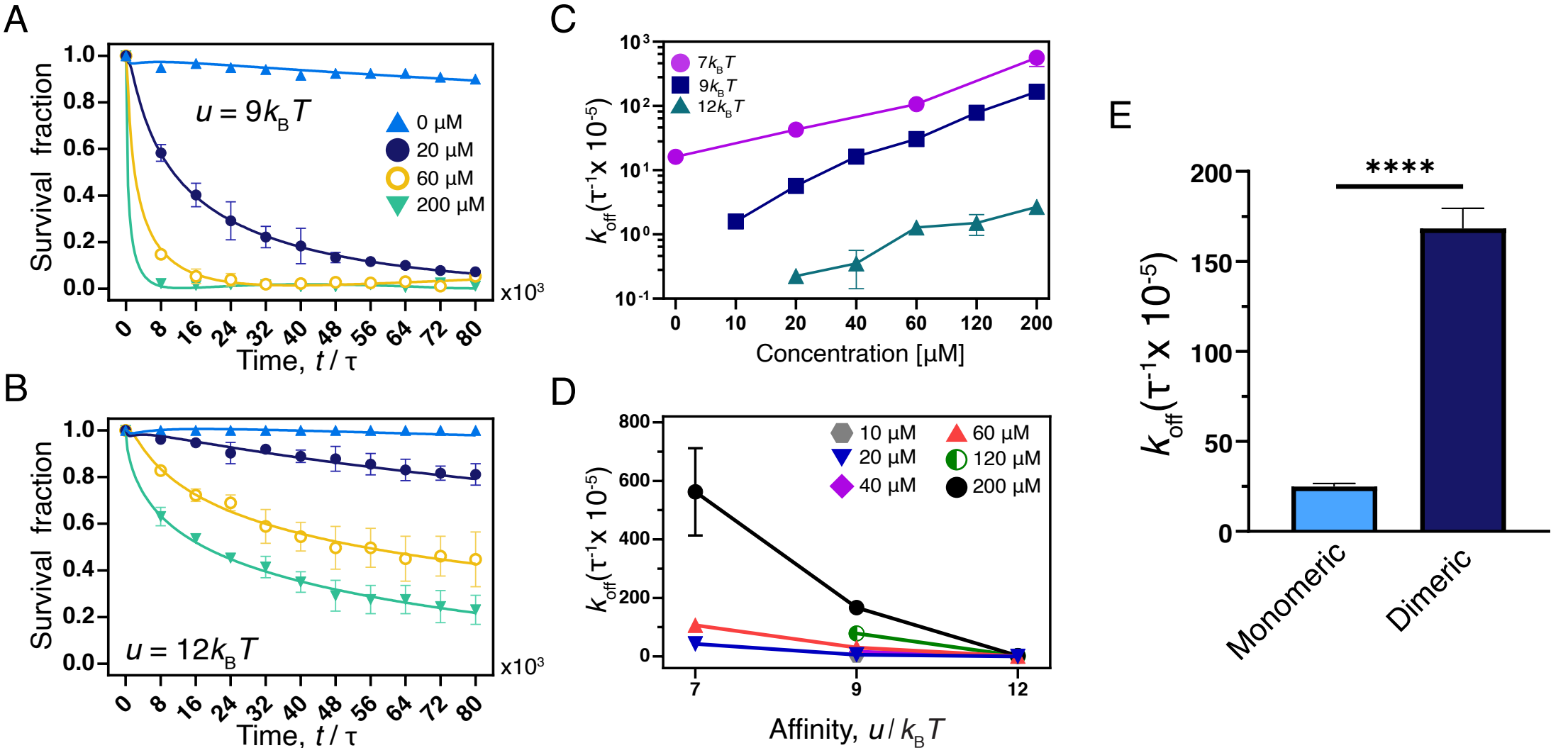
A
Survival fraction
1.0
0.8
0.6
0.4
0.2
0.0
$u = 9k_BT$
0 μM
20 μM
60 μM
200 μM
x10³
0 8 16 24 32 40 48 56 64 72 80
Time, t / τ
B
Survival fraction
$u = 12k_BT$
x10³
Time, t / τ
C
$7k_BT$
$9k_BT$
$12k_BT$
$k_{off}(\tau^{-1} \times 10^{-5})$
10^3
10^2
10^1
10^0
10^{-1}
0 10 20 40 60 120 200
Concentration [μM]
D
10 μM
20 μM
40 μM
60 μM
120 μM
200 μM
$k_{off}(\tau^{-1} \times 10^{-5})$
800
600
400
200
0
7 9 12
Affinity, u / k_BT
E
****
$k_{off}(\tau^{-1} \times 10^{-5})$
200
150
100
50
0
Monomeric
Dimeric

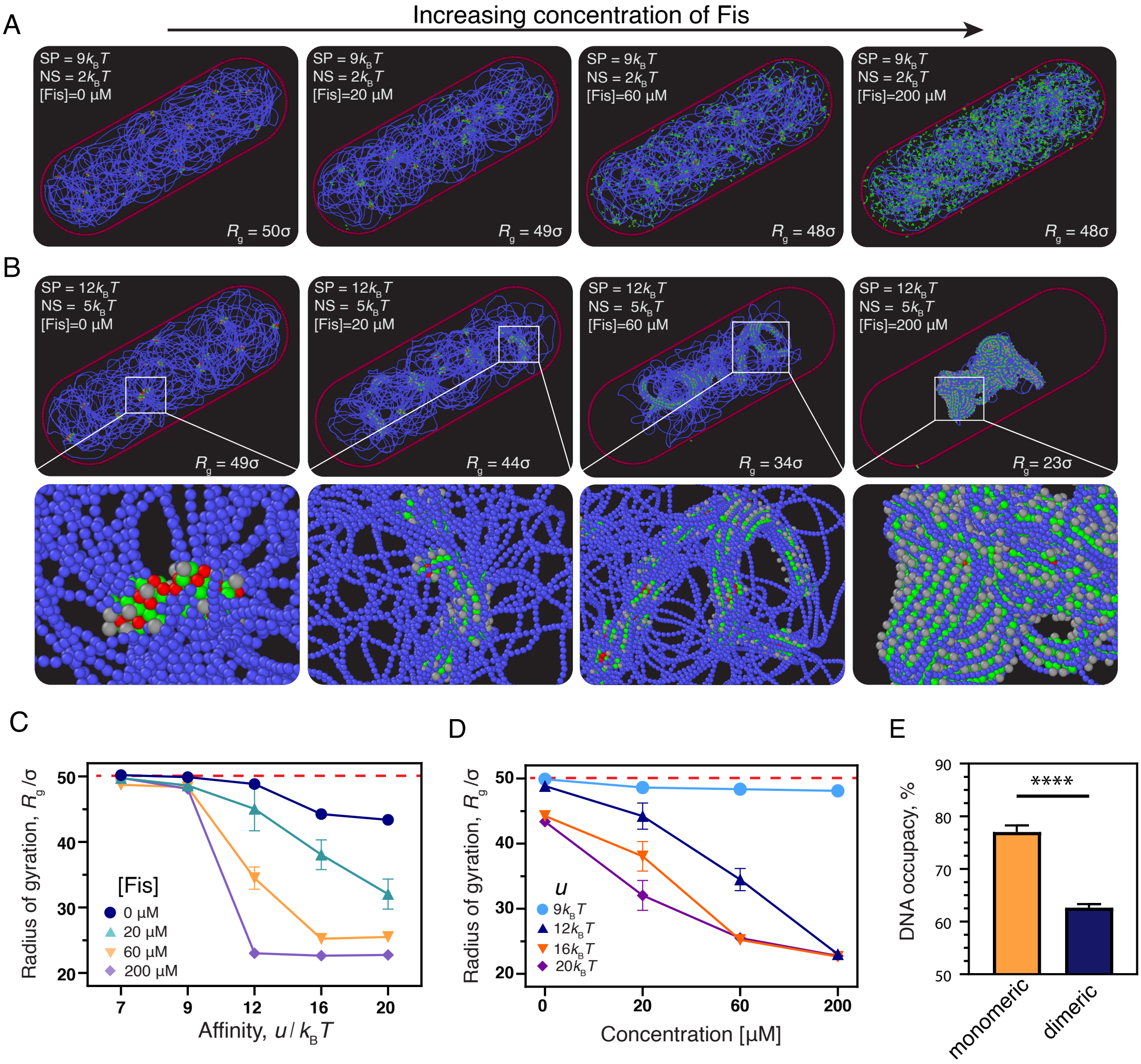
A
Increasing concentration of Fis
SP = 9k_BT
NS = 2k_BT
[Fis]=0 μM
R_g = 50σ
SP = 9k_BT
NS = 2k_BT
[Fis]=20 μM
R_g = 49σ
SP = 9k_BT
NS = 2k_BT
[Fis]=60 μM
R_g = 48σ
SP = 9k_BT
NS = 2k_BT
[Fis]=200 μM
R_g = 48σ
B
SP = 12k_BT
NS = 5k_BT
[Fis]=0 μM
R_g = 49σ
SP = 12k_BT
NS = 5k_BT
[Fis]=20 μM
R_g = 44σ
SP = 12k_BT
NS = 5k_BT
[Fis]=60 μM
R_g = 34σ
SP = 12k_BT
NS = 5k_BT
[Fis]=200 μM
R_g = 23σ
C
Radius of gyration, R_g/σ
50
40
30
20
[Fis]
0 μM
20 μM
60 μM
200 μM
7
9
12
16
20
Affinity, u / k_BT
D
Radius of gyration, R_g/σ
50
40
30
20
u
9k_BT
12k_BT
16k_BT
20k_BT
0
20
60
200
Concentration [μM]
E
DNA occupacy, %
90
80
70
60
50
****
monomeric
dimeric

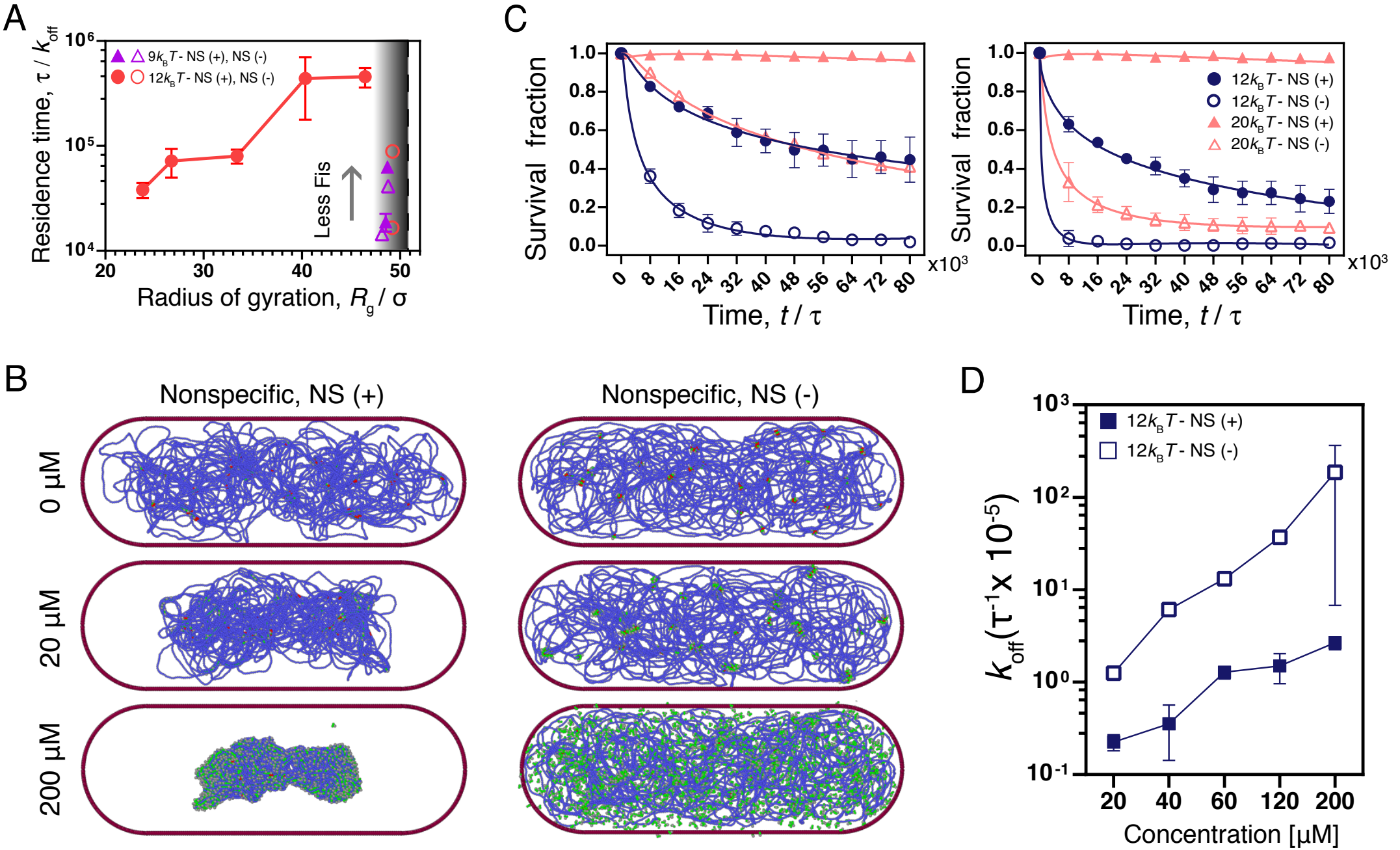
A
Residence time, τ / k_{off}
10^6
10^5
10^4
$9k_BT$- NS (+), NS (-)
$12k_BT$- NS (+), NS (-)
Less Fis
20
30
40
50
Radius of gyration, R_g / σ
C
Survival fraction
1.0
0.8
0.6
0.4
0.2
0.0
0
8
16
24
32
40
48
56
64
72
80
x10³
Time, t / τ
$12k_BT$- NS (+)
$12k_BT$- NS (-)
$20k_BT$- NS (+)
$20k_BT$- NS (-)
B
Nonspecific, NS (+)
Nonspecific, NS (-)
0 μM
20 μM
200 μM
D
10^3
10^2
10^1
10^0
10^{-1}
k_{off}(τ^{-1}x 10^{-5})
$12k_BT$- NS (+)
$12k_BT$- NS (-)
20
40
60
120
200
Concentration [μM]

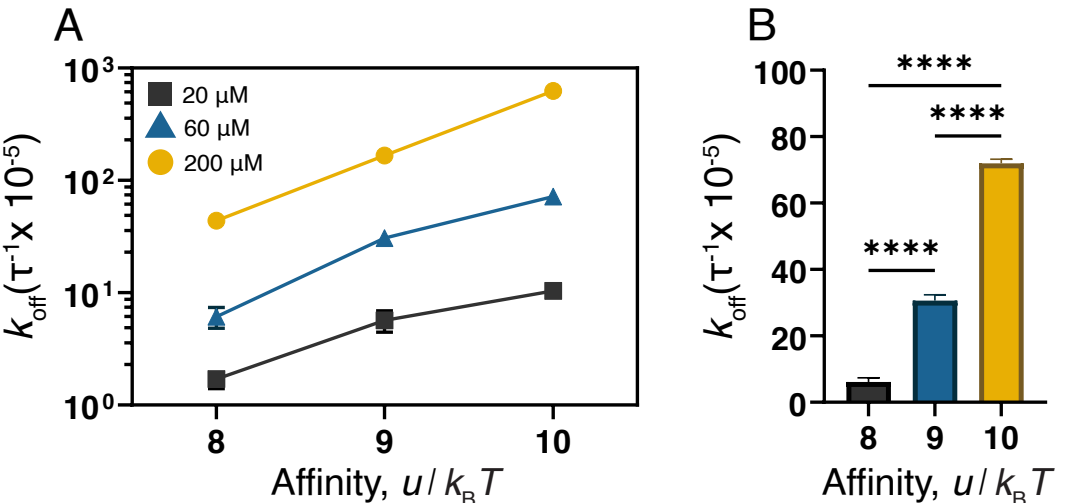
A
B
20 μM
60 μM
200 μM
10^3
10^2
10^1
10^0
$k_{off}(\tau^{-1} \times 10^{-5})$
8
9
10
Affinity, $u / k_B T$
****
****
****
100
80
60
40
20
0
$k_{off}(\tau^{-1} \times 10^{-5})$
8
9
10
Affinity, $u / k_B T$